Fire Safety Journal 153 (2025) 104354

Contents lists available at ScienceDirect

Fire Safety Journal

journal homepage: www.elsevier.com/locate/firesaf

Numerical investigation on the inhibition effect of HBr in stoichiometric hydrogen/air mixtures on head-on flame quenching (HoQ)☆

Chunkan Yu *, Robert Schießl

Institute of Technical Thermodynamics, Karlsruhe Institute of Technology, Engelbert-Arnold-Str. 4, Karlsruhe 76131, Germany

ARTICLE INFO

Keywords:
Head-on quenching
Flame inhibitor
Hydrogen bromide (HBr)
Flame/wall interaction

ABSTRACT

This paper investigates the effect of the flame retardant hydrogen bromide (HBr) on premixed hydrogen/air flames undergoing head-on quenching at an inert cold wall. Numerical simulations with full spatio-temporal resolution and detailed treatment of chemical reactions and molecular transport are employed to study this configuration. The simulations reveal how the addition of HBr affects the species profiles and the heat release rate in the flame, particularly at the quenching time, defined as the point of maximum heat loss to the wall. It is found that the accumulation of HO_2 and H_2O_2 at the wall, which is significant for pure hydrogen/oxygen flames, becomes much weaker in the presence of HBr. Instead, with HBr the near-wall accumulation of Br and Br_2 becomes more pronounced. Further investigation shows that the recombination reaction Br+Br+M → Br_2 + M is the dominant exothermic reaction contributing to the heat release rate at the wall. Moreover, heat losses from the flame to the wall have been compared for different fuels. For stoichiometric H_2 air, the wall heat loss (and therefore the thermal stress exerted onto the wall by the flame) is around two times higher than that for a conventional fuel like, e.g. methane. However, when 2% HBr are added to the combusting mixture, the heat loss is similar to methane. HBr addition can therefore efficiently reduce the thermal load for walls exposed to hydrogen combustion down to the levels of the conventional fuel CH_4.

1. Introduction

Hydrogen receives increasing attention for its potential role as a zero-carbon fuel in energy systems. A drawback in technological applications, however, is that hydrogen is highly flammable and explosive [1–3]. Means are desired to limit the high reactivity of hydrogen/air mixtures. This can be desirable for several reasons. From the aspect of explosion and fire safety, hydrogen can form flammable mixtures with air over a wide range of H_2/air ratios [1,2]. This flammability range is huge compared to that of most other fuels [4]. Therefore, hydrogen leaking from a pipe or a tank is a much more serious safety issue than a leaking conventional fuel [5,6]. Likewise, flames in hydrogen/air mixtures have a large propensity to transit to detonation, thus exacerbating the hazard potential of this fuel [7]. From the aspect of gas-phase combustion properties, a smooth transition from conventional fuels to carbon-free hydrogen strongly depends on the possibility of using existing (conventional fuel-based) combustion devices also with hydrogen fuel. The much higher flame speed of hydrogen compared to conventional fuels strongly changes the operation characteristics of combustion devices, like the required gas flow speed in turbines, flow patterns and cycle timing schemes in piston-based engines [8,9]. Availability of means for "tuning" the flame speed of hydrogen to match conventional fuels can render the fuel transition more seamless. From the aspect of flame/wall interaction, the properties of hydrogen flames allow hydrogen flames to sustain the heat release even when the flame is close to a solid surface [10], like the cylinder wall in an internal combustion engine or the surface of gas turbine blades [11,12]. This makes the thermal stress and high-temperature oxidation (corrosion) experienced by materials that get exposed to hydrogen flames much larger than the one experienced with other fuels (in particular, the "conventional" hydrocarbon fuels) [9,12]. This can impede re-fitting conventional (fossil fuel-based) combustion chamber hardware for operation with hydrogen, as special materials may be required to meet the stringent requirements of hydrogen combustion [9]. Means that allow to run conventional hardware with hydrogen are desired, and a reduction of hydrogen's reactivity to typical hydrocarbon fuel levels can aid this process.

Various studies have examined if and how addition of chemical substances to hydrogen/air mixtures can achieve the desired reduction

☆ This document is the result of the research project funded by the Deutsche Forschungsgemeinschaft (DFG).
* Corresponding author.
E-mail address: chunkan.yu@kit.edu (C. Yu).

https://doi.org/10.1016/j.firesaf.2025.104354
Received 8 January 2025; Received in revised form 5 February 2025; Accepted 13 February 2025
Available online 21 February 2025

of reactivity. Among the considered measures are adding diluents (e.g. N_2) [13,14], and also adding chemical inhibitors like H_2O and CO_2 [15,16], trifluoroiodomethane (CF_3I) [17], hydrofluorocarbons (e.g. CHF_3 and C_2HF_5) [18], bromine species (e.g. HBr and Br_2) [19–21], and aqueous solution [22]. Commonly used inhibitors include halogenated compounds, such as halons, which release halogen atoms that react with key radicals (H, O, and OH) in the flame, thereby interrupting the chain reactions essential for combustion. A review on suppression effects of various inhibitors (up to eighty compounds) on hydrogen-air flames can be found in e.g. [3,23,24].

Most studies concerning the effect of inhibitors on hydrogen/air systems primarily concentrate on the suppression effect on laminar premixed flames, specifically in terms of laminar burning velocity and explosion limits [17,18,20]. These studies provide valuable insights into the fundamental combustion characteristics and the effectiveness of various inhibitors in controlling flame propagation and stability. However, there are fewer investigations reporting the inhibitor effect on hydrogen/air systems interacting with walls and the consequent quenching processes. Flame-wall interactions (FWI) are of great interest in designing and developing new engineering applications. As is well-known, flames can be quenched by solid surfaces in a range of practically relevant combustion systems [25,26]. This quenching process is critical in understanding how inhibitors perform in real-world scenarios where flames often encounter physical boundaries. The interaction of flames with walls can significantly affect the flame structure, species profiles and the overall efficacy of flame inhibitors. Investigation of wall quenching can typically be divided into three different groups [27]: (i) the head-on quenching (HoQ) process, where flame propagation is perpendicular to the cold wall, (ii) side-wall quenching (SWQ), where the flame propagates parallel to the cold wall, and (iii) tube quenching, where the flame quenches inside a tube as it propagates. Various studies have shown that the flame-wall geometry plays a significant role in the quenching process, with intensive investigations conducted in, e.g., [28,29]. For HoQ, the configuration can be simplified to a one-dimensional flame geometry, enabling the study of parameters such as reaction mechanisms and mixture compositions with lower computational costs [30]. In contrast, SWQ or tube quenching requires a two-dimensional or three-dimensional numerical approach, which necessitates considering multidimensional diffusion transport [31] and boundary layer effects [29].

The present work investigates the head-on quenching (HoQ) process, describing flame-wall interaction in a one-dimensional geometry. Although the more complex multidimensional diffusion effects and other phenomena present in two- or three-dimensional geometries are not included in the one-dimensional HoQ process, this simplification allows for a computationally efficient approach. Consequently, parameter studies can be conducted at a lower computational cost while still providing valuable insights into the fundamental mechanisms of flame quenching. The impact of HBr as an inhibitor on the quenching process is studied in detail, focusing on the species profiles and heat release rate profiles. The phenomena are discussed in comparison with the quenching process of hydrogen/air flames without HBr doping.

2. Modeling for head-on quenching at an isothermal wall

In the present work, we simulate the processes during head-on quenching of a one-dimensional premixed hydrogen/air flame doped with HBr. Although the one-dimensional geometry is relatively simple, it proves to be a highly effective tool for investigating flame-wall interactions. This approach enables numerical simulations by using detailed transport models and comprehensive chemical kinetics. The use of the one-dimensional geometry is well-documented in the literature, where it has been extensively employed to study the head-on quenching process in one-dimensional geometry [27,32,33]. These studies demonstrate its capability to provide valuable insights into flame quenching dynamics, offering a robust framework for analyzing complex interactions in combustion systems while maintaining computational efficiency.

Table 1
Boundary conditions for the numerical simulation.

	Left boundary ($x = 0^+$)	Right boundary ($x = \Omega$)
Temperature:	$T = T_{ub} = T_w$	$\frac{\partial T}{\partial x} = 0$
Species mass flux	$\rho w_i V_i = 0$	(–)
Species mass fraction	(–)	$\frac{\partial w_i}{\partial x} = 0$
Pressure	$p = 1$ bar	$p = 1$ bar

Fig. 1 exemplifies the process by showing qualitative spatio-temporal profiles of temperature: The first stage (left figure) represents flame propagation towards an isothermal and non-reacting wall (located at $x = 0$ m) with a constant speed equal to the laminar burning velocity; The second stage (right figure) begins when the flame feels the presence of the wall due to heat loss. If the heat loss becomes sufficiently large, flame quenching occurs.

The amount of doped retardant HBr is expressed by the mole fraction X(HBr) of HBr in the unreacted mixture:

$$X(\mathrm{HBr}) = \frac{n(\mathrm{HBr})}{n(\mathrm{H_2}) + n(\mathrm{Air}) + n(\mathrm{HBr})} \tag{1}$$

where n_i is the molar amount of component i in the mixture ($i = 1, \ldots, n_s$, with n_s the total number of species).

Table 1 gives the relevant boundary conditions applied in our numerical simulation. The combustion system is isobaric at $p = 1$ bar. The species mass flux $j_i^s = \rho w_i V_i$ vanishes at the surface ($x = 0^+$), where V_i is the diffusion velocity. It should be emphasized that, in the present work, the wall surface temperature is assumed to be isothermal and remains unchanged throughout the analysis. However, as investigated in [34], the choice of wall materials and the application of thermal-barrier coatings can affect the quenching distance. Such findings open up potential further investigation, particularly for the considered combustion systems.

The initial condition for the flame is given by spatial profiles of a freely propagating flame in the gas phase, far away from the wall.

The employed chemical mechanism for H_2/air coupled with inhibition mechanism involving HBr consists of two sub-mechanisms: (i) a H_2/air mechanism from the Maas and Warnatz [35]; (ii) a Br/H/O sub-mechanism from the one developed by Dixon-Lewis et al. [20]. The mechanism consists of 15 species, which participate in 49 reversible elementary reactions.

The numerical simulation is performed by the in-house code *INSFLA* [35]. This code solves the unsteady conservation equations for energy, species and momentum in reacting flows in one spatial dimension with detailed chemistry and detailed transport model including differential diffusion and thermal diffusion (Soret effect) [36]. The numerical solution method features a self-adapting spatial grid system and time stepping with error control. The INSFLA code has been extensively validated against experiments for various fundamental combustion properties, including ignition delay time [37], explosion limit [35], laminar flame speed [38], extinction strain rate [39], and minimum ignition energy [40]. For the considered HoQ process studied in the present work, INSFLA has also been validated against experimental measurements by comparing species concentrations with and without considering wall surface reactions [41,42].

Fig. 2 compares simulated and measured values of the laminar burning velocity (LBV) in dependence of X(HBr). As observed in prior studies [20], HBr addition decelerates LBV. This phenomenon is attributed to the interaction of bromide Br with the radicals H and HO_2, as studied by sensitivity analysis in [20]. In presence of Br, these species undergo chain termination reactions, yielding stable Br_2 and HBr molecules:

$$\mathrm{H + Br + M \rightleftharpoons HBr + M}$$

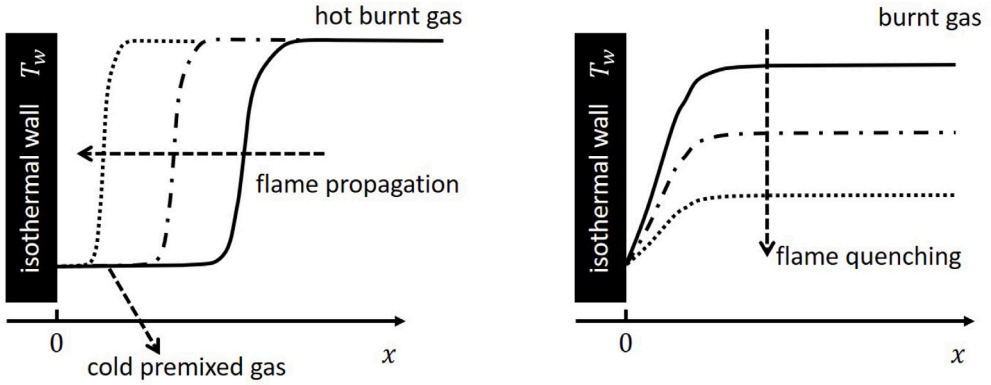

Fig. 1. Schematic illustration of Head-on Quenching (HoQ) process in the present work.

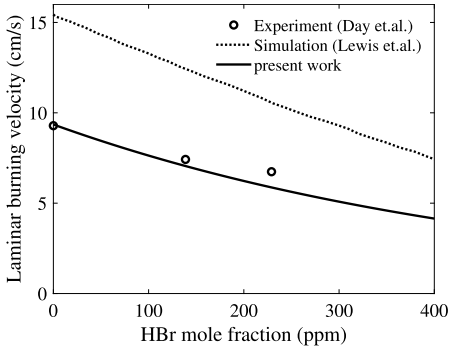

Fig. 2. Measured and computed laminar burning velocity versus HBr in mole fraction (ppm). Experiment measurement from Day et al. [43], simulation from Lewis et al. [20]. Inlet gas composition was 18.8% H_2, 4.6%O_2 and 76.6%N_2 by mole, with varying amounts of HBr.

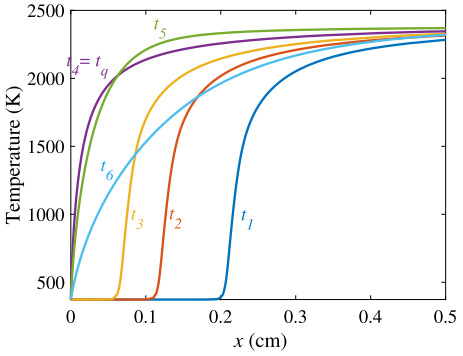

Fig. 3. Transient temperature profiles for stoichiometric H_2/air premixed flame with 4% mole fraction HBr addition. Different lines represent various time points with $t_1 < t_2 < t_3 < t_4 = t_q < t_5 < t_6$.

$$Br + Br + M \rightleftharpoons Br_2 + M$$

$$Br + HO_2 \rightleftharpoons HBr + O_2$$

This removal of radicals retards further progress of chemical reaction in the flame's reaction zone, and thereby reduces the laminar burning velocity.

3. Results and discussion

In the following, the transient head-on quenching process of premixed stoichiometric hydrogen/air added with HBr at $p = 1$ bar will be discussed. The computational domain is 5 cm, and the flame front of the unstrained freely propagating flame is located at around 4 cm. This positioning ensures that the flame is far from the cold wall, meaning there is no initial effect of the cold wall on the premixed flame.

The range $0 \leq X(\mathrm{HBr}) \leq 6\%$ of HBr doping is considered in this work, which is consistent with the range in [20]. As shown in this work, the addition of 6% HBr to a hydrogen/air mixture significantly reduces the laminar flame speed by approximately 80% compared to that of a hydrogen/air mixture without HBr. Moreover, this addition results in a laminar flame speed similar to that of a methane/air premixed flame. Thus, adding 6% HBr to a hydrogen/air mixture results in a strong inhibition effect in terms of laminar flame speed, enhancing process safety. Consequently, this concentration range is worth investigating to examine the corresponding inhibition effect during the quenching process.

The transient species profiles and heat release rate profiles will be studied in detail. Specifically, we will analyze how the addition of HBr influences the formation and quenching of key species such as HO_2, H_2O_2 (which are important for the hydrogen/oxygen premixed flame interacted with wall [10]) as well as the overall heat release rate. Additionally, the accumulation behavior of Br and Br_2 at the wall will be examined, highlighting the distinct mechanisms governing their concentrations during the quenching process.

3.1. Temperature profile analysis

To initiate the discussion, Fig. 3 presents typical transient profiles of temperature for a stoichiometric H_2/air premixed flame with 4% mole fraction HBr addition. The isothermal non-reacting wall with $T_w = 373$ K is positioned at $x = 0$, and the flame propagates freely from t_1 until t_3. As the flame approaches the wall more closely, the temperature gradient at the wall rises rapidly. At the time where the heat loss at the wall reaches its maximum ($t_4 = t_q$), the flame is quenched. Afterwards, the temperature tends to the cold wall temperature until the temperature is spatially homogeneous throughout the entire domain.

Fig. 4 (left) further shows the spatial temperature profiles for flames with different HBr additions at quenching times, where the heat loss at the wall reaches its maximum. It is observed that the temperature gradients at the wall decrease monotonically with increasing HBr additions. Consequently, the heat loss at the wall at the quenching time is reduced by approximately 80% with the addition of just 6% HBr to the mixtures, which can be observed in Fig. 4 (right).

It should also be mentioned at this point that for the same configuration, the laminar premixed methane/air flame results in heat loss at the wall with a maximum of 0.75 MW/m^2 [42]. Such amount of heat loss can also be achieved for hydrogen/air system doping with only 2%. If 6% HBr is added into the system, the heat loss at the wall is around 0.2 MW/m^2, which is lower than the heat loss caused by the premixed iso-octane/air flame with a maximum of 0.3 MW/m^2 [44].

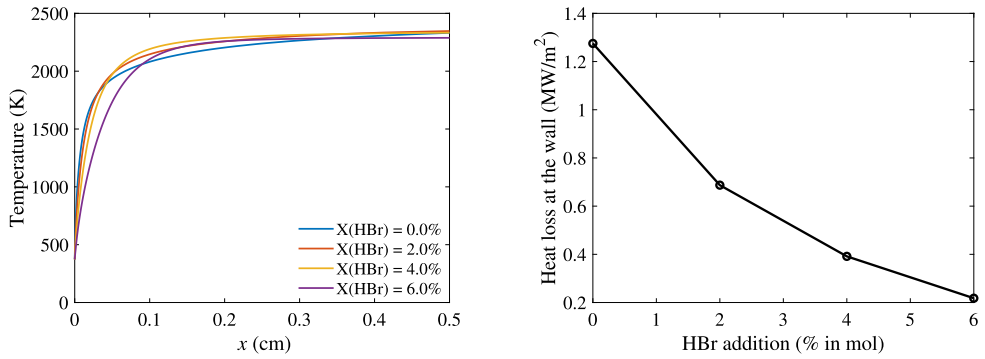

Fig. 4. Left: spatial temperature profiles for flame with different HBr additions at quenching times. Right: dependence of max. heat loss at the wall against HBr addition in the gas mixture.

3.2. Species profile analysis

3.2.1. H, O, OH, HO_2 and H_2O_2

As Dabireau et al. [10] reports in detail, for a premixed H_2/O_2 flame interacting with an inert wall, the profiles of the radicals H, O and OH across the flame front remain almost unchanged relative to a freely propagating flame until quenching sets in. The low temperature levels at cold walls prevent chain branching reactions of these radicals. However, HO_2 and H_2O_2 get accumulated at the wall surface since they are produced at the low temperatures near the wall by several recombination reactions. Such reactions are

$$H + O_2 + M \rightarrow HO_2 + M$$

and $$HO_2 + HO_2 \rightarrow H_2O_2 + O_2$$

This is also seen in Fig. 5, which shows mole fraction-vs.-temperature profiles of H, HO_2 and H_2O_2 (right) for H_2/air flames without HBr addition ($X(\mathrm{HBr}) = 0$, upper row) and with 4% HBr addition ($X(\mathrm{HBr}) = 4\%$, lower row). Showing the profiles vs. temperature (rather than vs. the distance from the wall) more clearly highlights some important features. Each row compares steady, freely propagating H2/air flames (blue profiles) with head-on quenching flames (red). These results for pure H_2/air flames are consistent with those of Dabireau et al. [10], showing that HO_2 and H_2O_2 accumulate at the cold wall surface (373 K), leading to relatively high mole fractions compared to those in freely propagating flames.

This phenomenon is not observed in flames with HBr addition. Comparison of the upper and lower row in Fig. 5 shows that mole fractions of HO_2 and H_2O_2 for the case $X(\mathrm{HBr}) = 4\%$ are one to two orders of magnitude below those for the case $X(\mathrm{HBr}) = 0$. As discussed in [20], the presence of HBr enables the chain termination step

$$Br + HO_2 \rightarrow HBr + O_2$$

which reduces the flame speed, and significantly consumes HO_2. The reduction of HO_2 levels leads to a reduction of H_2O_2 levels. Therefore, in HBr doped flames, HO_2 and H_2O_2 cannot significantly accumulate at the wall, in contrast to pure hydrogen flames, with a wall, as pointed out in [10].

Investigating the formation rate of HO_2 and H_2O_2 at the wall at the quenching time, it is shown that the major HO_2-consuming reaction is the chain termination step

$$Br + HO_2 \rightarrow HBr + O_2 \quad ,$$

which keeps HO_2 at the wall at a low level. On the other hand, a slight accumulation of H_2O_2 at the wall at the quenching time is observed, which can be attributed to the reaction

$$HBr + HO_2 \rightarrow Br + H_2O_2 \quad .$$

3.2.2. Br and Br_2

Fig. 6 represents typical transient mole fraction profiles for Br and Br_2 for stoichiometric H_2/air premixed flame with 4% mole fraction HBr addition. The timepoints corresponds to those in temperature profiles in Fig. 3. It is clearly observed that the main feature is the accumulation of Br and Br_2 directly at and near the cold wall. In other words, concentrations of both Br and Br_2 at the wall will increase when the flame gets closer to the wall and is affected by it. Afterwards they decrease again.

To demonstrate this phenomenon more clearly, in Fig. 7 we show the relationship between mole fractions of Br and Br_2 against temperature at two specific timepoints: when the flame is freely propagating (blue lines) and at the quenching time (red lines), which corresponds to the moment of maximum heat loss flux at the wall. Like in Fig. 5, showing the profiles vs. temperature (rather than vs. the distance from the wall) more clearly highlights some important features. It is seen that while the temperature brings similar concentrations of Br and Br_2 at high temperature ranges, the concentration profiles look quite different for both timepoints at low to middle temperature ranges. Especially at the temperature 373 K where the cold wall is located, both Br and Br_2 are accumulated and the Br_2 concentration at the wall can be even around seven times higher than its peak value in the freely propagating flame.

To investigate the accumulation of both species at the wall, Fig. 8 shows the temporal development of Br and Br_2 at the wall surface (red solid lines). It is clearly seen that both species' concentrations increase significantly and rapidly to a peak, and then decrease due to flame quenching. Analyzing the diffusive transport rate and chemical reaction rate, it is interesting to note that the controlling factors for species accumulation are totally different for each species:

- For atomic Br, the chemical source term is negative throughout the entire transient process, i.e., atomic Br is chemically consumed at the wall surface. Thus, the accumulation of Br is by the (positive) diffusive transport term.
  Atomic Br quickly diffuses from the reaction zone in the flame to the wall, due to its high concentration gradients pointing towards the wall (c.f. Fig. 6 (left)).
- Molecular Br_2 has a positive chemical source term at the wall throughout the whole transient process. This positive source term is dominant over the diffusive transport term, making chemical production the controlling factor for the accumulation of Br_2.

Now the remaining question is which elementary reactions mainly contribute to the consumption or production of Br and Br_2. To answer this question, the total reaction of production (ROP) and the ROP of each elementary reactions are computed for both Br and Br_2, and the contribution of each elementary reaction to the total ROP is calculated. The 6 elementary reactions with largest contribution are presented in

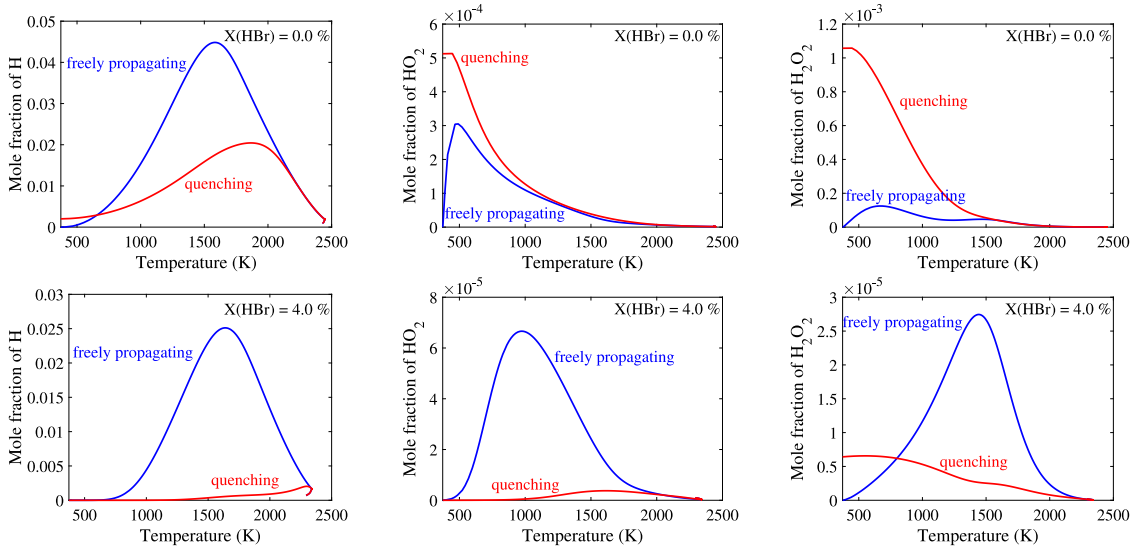

Fig. 5. Mole fractions of H (left), HO_2 (middle) and H_2O_2 (right) versus temperature for steady freely propagating flames (blue) and quenching flames (red) for pure hydrogen/air system (upper, X(HBr) = 0.0%) and hydrogen/air with 4% HBr addition (lower, X(HBr) = 4.0%). (For interpretation of the references to colour in this figure legend, the reader is referred to the web version of this article.)

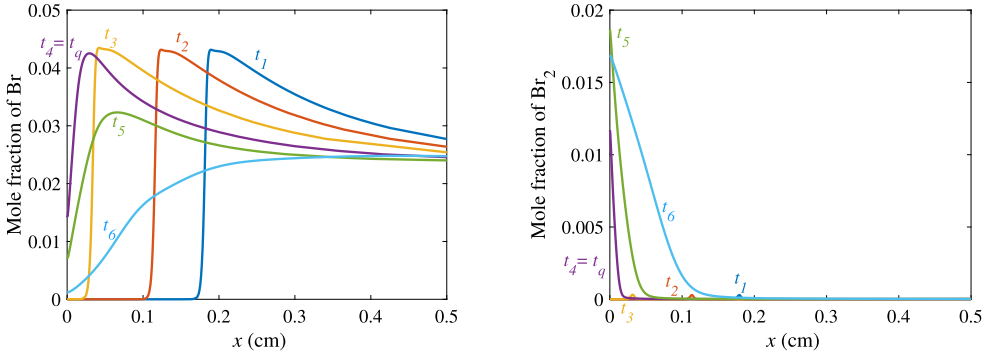

Fig. 6. Transient mole fractions of Br and Br_2 profiles for stoichiometric H_2/air premixed flame with 4% mole fraction HBr addition. Timepoints are the same as in Fig. 3.

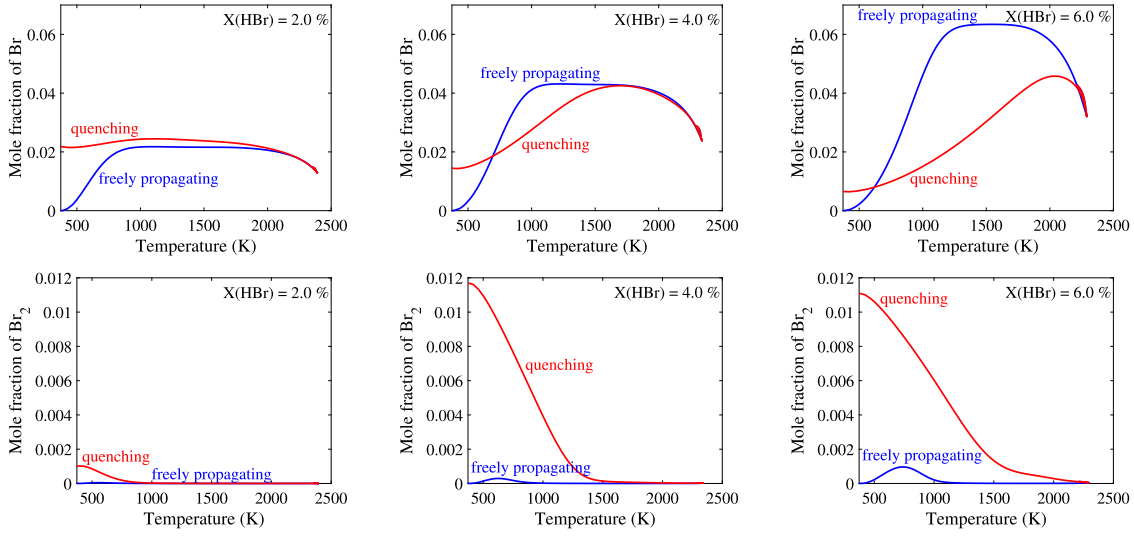

Fig. 7. Mole fractions of Br (upper) and Br_2 (lower) versus temperature for HBr-doped stoichiometric atmospheric H_2/air systems, for steady freely propagating flames (blue) and quenching flames (red), at different levels of HBr addition (mole percent in fuel/air mixture). (For interpretation of the references to colour in this figure legend, the reader is referred to the web version of this article.)

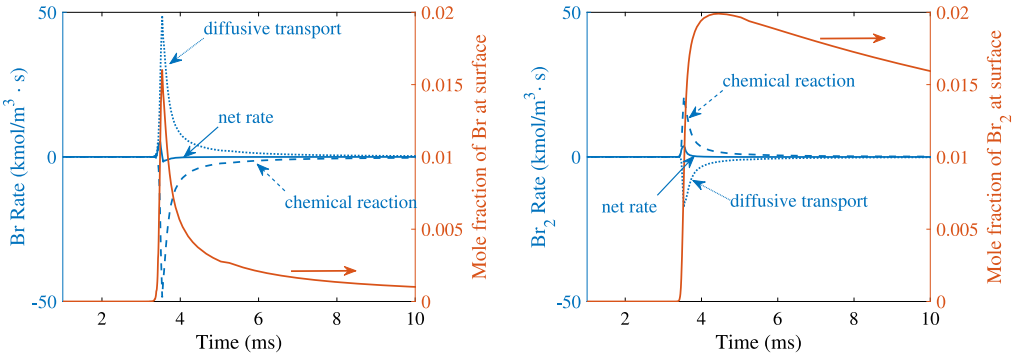

Fig. 8. Time development of change rate of Br (left) and Br_2 (right) and of mole fraction of species at the wall surface for stoichiometric H_2/air premixed flame with 4% mole fraction HBr addition. Blue dashed curves: Rate of change (ROC) due to chemical reaction; Blue dotted curves: Rate of change (ROC) due to molecular transport; Blue solid curves: the resulting net ROC. Red: Mole fraction profiles. (For interpretation of the references to colour in this figure legend, the reader is referred to the web version of this article.)

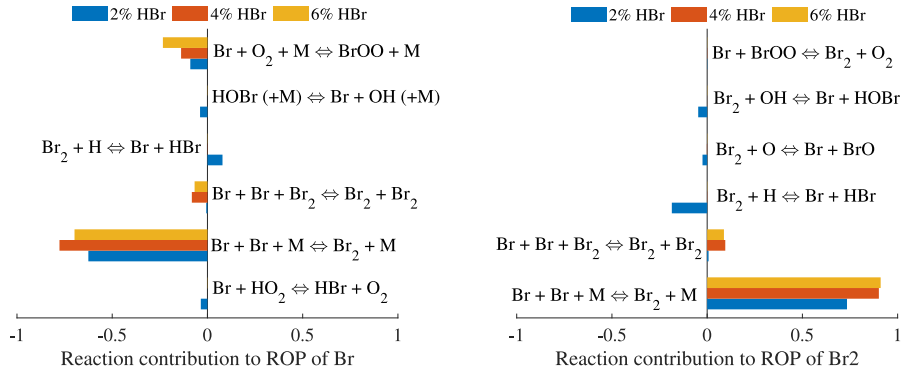

Fig. 9. Contribution $C_{is,jr}$(ROP) of the six most important reactions to production or consumption of Br and Br_2 at the wall at the quenching time $t = t_q$. Yellow, red and blue bars represent different levels of HBr addition to H_2/air flames, as indicated in the legend. (For interpretation of the references to colour in this figure legend, the reader is referred to the web version of this article.)

Fig. 9. In this figure, the reaction contribution is defined as

$$C_{is,jr}(\mathrm{ROP}) = \frac{\dot{\omega}_{is,jr}}{\sum_{jr=1}^{n_r} \left|\dot{\omega}_{is,jr}\right|}, \tag{2}$$

in which index is identifies species, and jr identifies elementary reactions. n_r is the total number of elementary reactions. $\dot{\omega}_{is,jr}$ represents the reaction rate of the jrth chemical reaction for the isth species. Negative (positive) values of $C_{is,jr}$(ROP) indicate that reaction jr contributes to the consumption (production) of species is, respectively.

The figure shows that for all three levels of HBr addition, the recombination reaction

$$\mathrm{Br + Br + M \rightarrow Br_2 + M}$$

is the most important elementary reaction contributing to the consumption of Br and to the production of Br_2.

3.2.3. BrOO, HOBr and BrO

In this part, the remaining three species, BrOO, HOBr and BrO, will be shortly discussed. As will be shown later, these three species are less important since they are all in low concentrations and have only minor contribution to the heat release rate.

Fig. 10 shows the mole fractions of BrOO (left), HOBr (middle) and BrO (right) versus temperature for steady, freely propagating flames (blue) and for quenching flames (red) for hydrogen/air systems with 4% HBr addition.

It is firstly observed that the BrOO concentration is at a very low level. This has also been observed in [20], which shows that the BrOO mole fraction tends to zero due to the low thermal stability of this species. The bond strength of Br-OO is estimated to be 1.7 ± 3.9 kJ/mol, which is essentially zero, indicating that BrOO is not a stable species. This low stability leads to negligible levels of BrOO, making it an insignificant factor in the H_2/air/HBr system under the studied conditions.

This is also the case for HOBr, which is present only at very low mole fraction levels. As discussed in [20], HOBr was not even considered in early work on inhibition by bromine species, as it is not important for the generation or removal of chain carriers under the considered conditions. The negligible impact of HOBr further simplifies the analysis of bromine's role in flame inhibition and quenching, since it also has almost no contribution to the heat release rate (see below).

Finally, BrO profiles are shown in Fig. 10. They indicate that, although BrO also exists only at low mole fraction levels, it accumulates at the wall surface. At the quenching time, the BrO mole fraction at the wall surface is even by 50% higher than its peak value during free flame propagation. Fig. 11(left) shows the transient mole fraction of BrO profiles, and (right) the temporal development of the net rate of change of BrO at the wall surface.

The result indicates a dynamic process where BrO is initially formed mainly due to chemical reaction, simultaneously diffusing towards the wall. Over time, the concentration of BrO at the wall decreases, likely by both chemical consumption and further diffusion away from the wall. However, despite that such accumulation and subsequent reduction of BrO highlights the complex interaction between diffusion and chemical reactions, both the chemical reaction rate and diffusive transport rate are in a low level. Since the chemical reaction rate alters from positive (production of BrO) to negative (consumption of BrO), Fig. 12 shows the reaction contribution to the ROP of BrO at the time

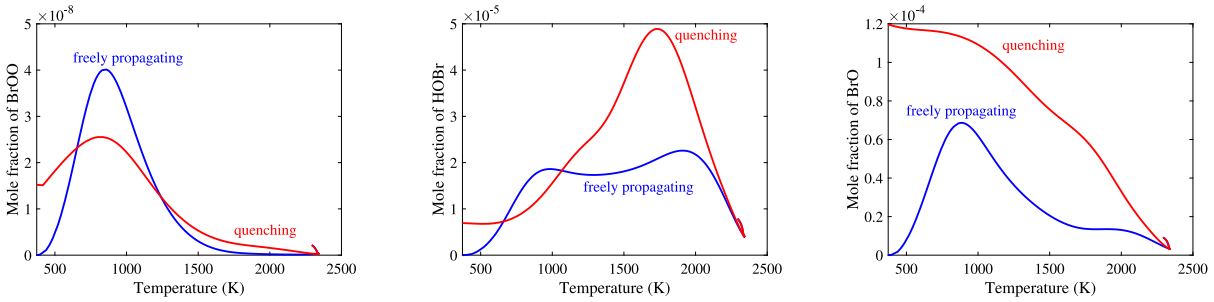

Fig. 10. Mole fractions of BrOO (left), HoBr (middle) and BrO (right) vs. temperature for steady freely propagating flames (blue) and quenching flames (red) with $X(\mathrm{HBr}) = 4\%$. (For interpretation of the references to colour in this figure legend, the reader is referred to the web version of this article.)

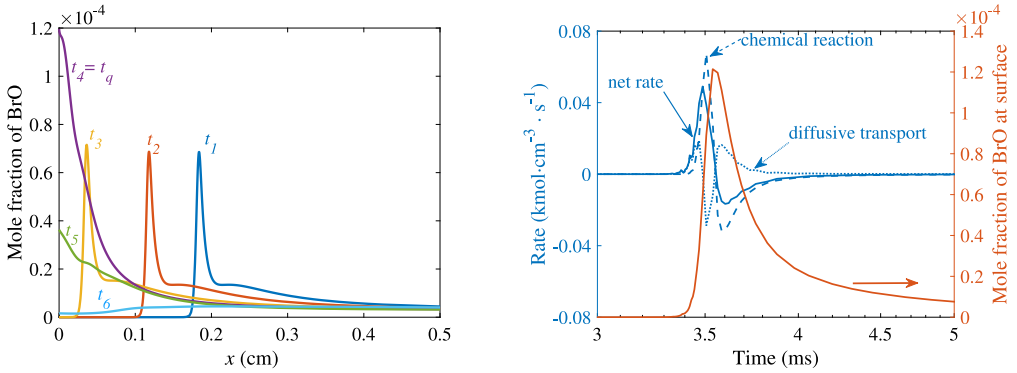

Fig. 11. Left: Transient mole fraction profiles of BrO for stoichiometric $X(\mathrm{HBr}) = 4\%$ flames. Right: Temporal evolution of several quantities for BrO at the wall surface ($x = 0$). Blue curves: Rate of change (ROC) due to chemical reaction, due to molecular transport, and the resulting net ROC. Red: Mole fraction of BrO. Timepoints are the same as in Fig. 3. (For interpretation of the references to colour in this figure legend, the reader is referred to the web version of this article.)

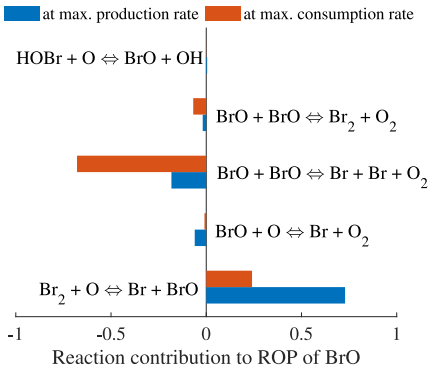

Fig. 12. Reaction contribution to the reaction of production (ROP) of BrO for hydrogen/air with 4% HBr addition at max. production reaction rate (blue) and at max. consumption rate (red). (For interpretation of the references to colour in this figure legend, the reader is referred to the web version of this article.)

of max. production reaction rate (blue bars) and of max. consumption reaction rate (red bars). It is clearly observed that the elementary reaction

$$\mathrm{Br_2 + O \rightarrow Br + BrO}$$

contributes dominantly to the production of BrO, and the reaction

$$\mathrm{BrO + BrO \rightarrow Br + Br + O_2}$$

mainly contributes to the consumption of BrO.

3.3. Heat release rate analysis

Following the discussion on species profile analysis, in this section we will focus on the analysis of the heat release rate (HRR), which is defined as:

$$\text{Heat release rate (HRR)} = -\sum_{i=1}^{n_s} \dot{\omega}_i h_i, \tag{3}$$

where $\dot{\omega}_i$ and h_i are the net production rate and specific enthalpy of species i $(i = 1 \ldots, n_s)$. The HRR is a crucial parameter for the dynamics of the combustion process, as it directly relates to the intensity and stability of the flame. Analyzing the HRR profiles during the transient quenching process of premixed hydrogen/air flames with varying HBr additions provides insight into the influence of HBr on the combustion characteristics.

Fig. 13 (left) shows transient HRR profiles for a stoichiometric hydrogen/air premixed flame with 4% HBr addition as an example, and (right) represents the corresponding temporal evolution of HRR at the wall surface. A closer look at the heat release rate (HRR) profiles reveals notable differences between the freely propagating flame (here $t_1 \ldots t_3$) and the quenching flame (here $t_4 = t_q \ldots t_6$): When flame quenching sets in ($t = t_4 = t_q$), the HRR-profile rapidly develops a pronounced peak directly at the wall. Afterwards, the flame temperature decreases and the corresponding HRR decreases simultaneously.

In Fig. 14, we show the relationship between heat release rate (HRR) and temperature at two specific points in time, one during free flame propagation (red) and the other at the quenching time t_q. As shown, the peaks of HRR for the freely propagating flames are located near 1000 K, whereas the HRR at quenching reaches its maximum at the isothermal wall. This observation clearly indicates a significant difference in the controlling chemistry for the two cases. Thus it is now of great interest to know which elementary reactions make the most contribution to the HRR.

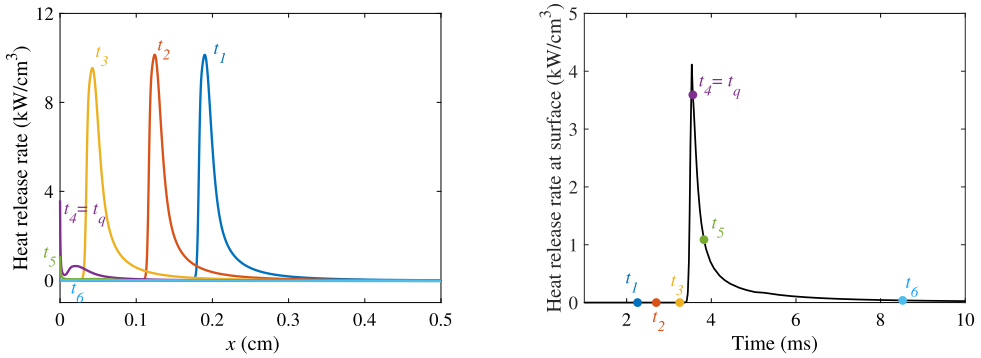

Fig. 13. Left: Transient HRR profiles for stoichiometric $X(\mathrm{HBr}) = 4\%$ doped hydrogen/air flames. Right: Temporal evolution of HRR at the wall surface ($x = 0$). Timepoints are the same as in Fig. 3.

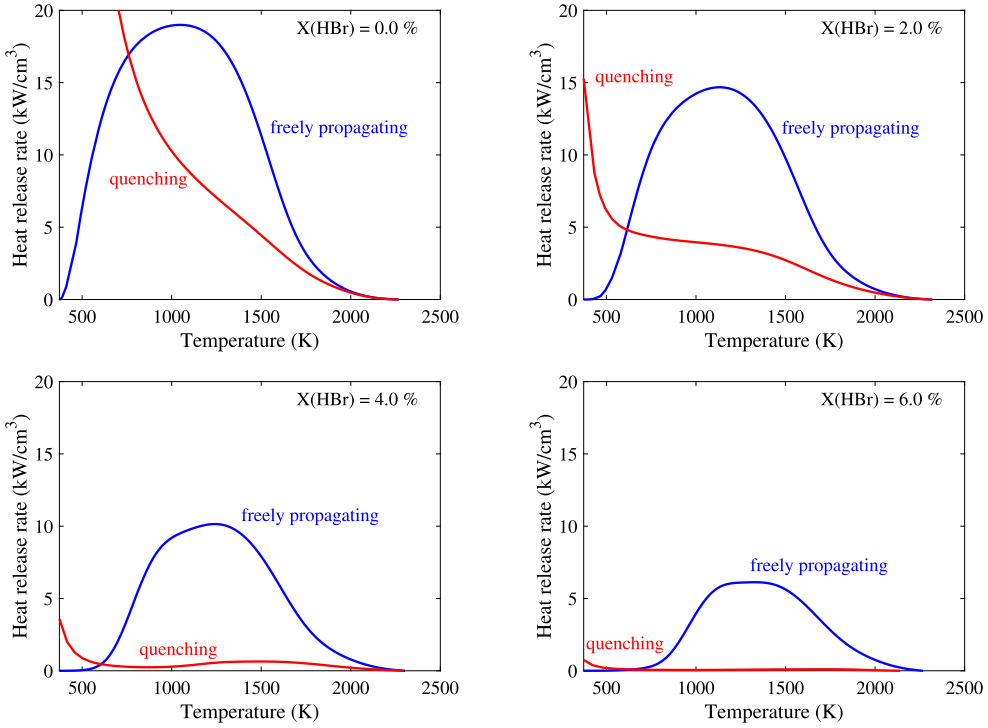

Fig. 14. Heat release rate versus temperature for steady freely propagating flames (blue) and quenching flames (red), with different levels of HBr addition given in mole percent in total mixture. (For interpretation of the references to colour in this figure legend, the reader is referred to the web version of this article.)

Fig. 15 shows the seven most important heat releasing reactions. Data for a freely propagating flame at the spatial peak of HRR are shown on the left, and data for a quenching flame ($t = t_q$) at the wall surface are shown on the right. It is evident that the main HRR-controlling reactions are different for the two cases: For the freely propagating flame, HRR is dominated by the reactions

$$H_2 + OH \Leftrightarrow H + H_2O,$$

$$H + O_2 + M \Leftrightarrow HO_2 + M,$$

and

$$H + HO_2 \Leftrightarrow OH + OH.$$

These reactions, however, become less important for the HRR at the wall surface in a quenching flame.

For a quenching flame, the recombination

$$H + O_2 + M \Leftrightarrow HO_2 + M$$

is important for a flame of pure hydrogen/air. In the presence of HBr, however, the production of atomic Br through the dissociation of HBr adds a new pathway for heat release. The recombination of atomic Br to form Br_2

$$Br + Br + M \Leftrightarrow Br_2 + M,$$

a highly exothermic process, results in a considerable heat release at the wall.

4. Summary and conclusions

This work analyzes the influence of the flame retardant hydrogen bromide (HBr) on laminar premixed hydrogen/air flames. A focus is the influence of HBr-addition on flame-wall interaction. The study is based on numerical simulations of laminar flames featuring detailed chemistry and transport. Simulations of flame-wall interaction with various

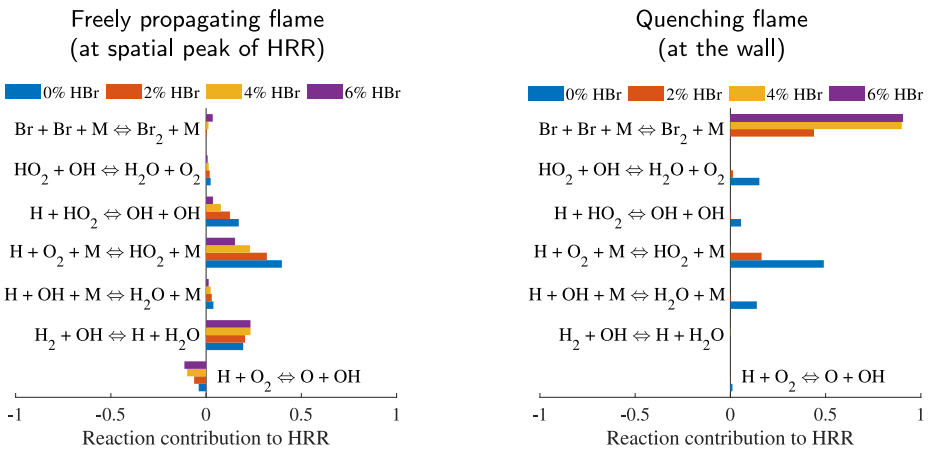

Fig. 15. The seven reactions contributing most to HRR for a freely propagating flame at the location of maximum heat release (left), and for a quenching flame at the wall surface. Blue, red, yellow and purple bars represent different levels of HBr addition to H_2/air flames, as indicated in the legend. (For interpretation of the references to colour in this figure legend, the reader is referred to the web version of this article.)

amounts (0% up to 6% by mol) of HBr are considered. The results yield insights on the impact of bromine species on flame behavior. Analysis of the transient spatial profiles of species and heat release rate (HRR) highlights how HBr addition affects the chemical reactions, diffusion processes and heat losses at the wall. The main results are as follows:

- Generally, when a flame front approaches a cold wall, the heat flux from the flame to the wall first increases, and the flame quenches by this large heat loss. This heat flux from the flame into the wall is significantly smaller for HBr-doped H_2/air mixture than for pure H_2/air: With solely 2% HBr addition, the resulting wall heat loss is similar to conventional hydrocarbon fuels such as methane and iso-octane. This reduction of the wall heat flux is particularly notable because it helps mitigating thermal stresses on the wall, which can lead to material degradation.
- During flame wall-interaction, HO_2 and H_2O_2 accumulate to high concentration levels at the wall. This accumulation is much lower for HBr-doped H_2/air compared to pure H_2/air.
- With HBr addition, atomic Br and molecular Br_2 accumulate at the wall to high amounts during flame-wall interaction. While the accumulation of Br can be attributed to diffusive transport from the flame front to the wall, the accumulation of Br_2 is due to chemical reactions. At the wall, the recombination reaction $Br + Br + M \rightarrow Br_2 + M$ is the dominant reaction contributing to the consumption of Br and the production of Br_2.
- Species HOBr and BrOO are present only at negligibly low concentration levels at the wall, and do not affect the flame behavior at the wall to any significant extent.
- Species BrO accumulates at the wall during flame-wall interaction to a relatively high level. BrO is initially produced by the reaction $Br_2 + O \rightarrow Br + BrO$, and then consumed by the reaction $BrO + BrO \rightarrow Br + Br + O_2$.
- At the flame quenching time, the heat release rate (HRR) profile reaches its maximum at the isothermal cold wall. The recombination reaction of atomic Br, $Br + Br + M \Leftrightarrow Br_2 + M$, then becomes the dominant exothermic reaction, significantly contributing to the heat release rate at the wall surface.

The present work provides insight into the impact of HBr on hydrogen/air flames interacting with a cold wall. This detailed analysis provides also a deeper understanding of how inhibitors like HBr can be utilized to control flame behavior and improve combustion usage in engineering applications. Noticeable accumulation of different species at the wall surface could potentially lead to heterogeneous wall reactions. In the future, surface reactions describing the recombination and destruction of radicals will be accounted for, and their possible effects on the quenching process will be further investigated.

CRediT authorship contribution statement

Chunkan Yu: Writing – original draft, Visualization, Validation, Software, Methodology, Investigation, Formal analysis, Conceptualization. **Robert Schießl:** Writing – review & editing, Methodology, Investigation, Formal analysis, Conceptualization.

Declaration of competing interest

The authors declare that they have no known competing financial interests or personal relationships that could have appeared to influence the work reported in this paper.

Acknowledgments

Authors acknowledge financial support by the DFG, Germany (project H2MA
T3D, project number 523879740 within the DFG-SPP 2419 HyCAM).

Data availability

Data will be made available on request.

References

[1] A.L. Sánchez, F.A. Williams, Recent advances in understanding of flammability characteristics of hydrogen, Prog. Energy Combust. Sci. 41 (2014) 1–55.
[2] D.A. Crowl, Y.-D. Jo, The hazards and risks of hydrogen, J. Loss Prev. Process. Ind. 20 (2) (2007) 158–164.
[3] M. van Wingerden, T. Skjold, D. Roosendans, A. Dutertre, A. Pekalski, Chemical inhibition of hydrogen-air explosions: Literature review, simulations and experiments, Process. Saf. Environ. Prot. 176 (2023) 1120–1129.
[4] K.L. Cashdollar, I.A. Zlochower, G.M. Green, R.A. Thomas, M. Hertzberg, Flammability of methane, propane, and hydrogen gases, J. Loss Prev. Process. Ind. 13 (3–5) (2000) 327–340.
[5] H. Li, X. Cao, Y. Liu, Y. Shao, Z. Nan, L. Teng, W. Peng, J. Bian, Safety of hydrogen storage and transportation: An overview on mechanisms, techniques, and challenges, Energy Rep. 8 (2022) 6258–6269.
[6] Y. Liang, X. Pan, C. Zhang, B. Xie, S. Liu, The simulation and analysis of leakage and explosion at a renewable hydrogen refuelling station, Int. J. Hydrog. Energy 44 (40) (2019) 22608–22619.
[7] F. Yang, T. Wang, X. Deng, J. Dang, Z. Huang, S. Hu, Y. Li, M. Ouyang, Review on hydrogen safety issues: Incident statistics, hydrogen diffusion, and detonation process, Int. J. Hydrog. Energy 46 (61) (2021) 31467–31488.
[8] P. Chiesa, G. Lozza, L. Mazzocchi, Using hydrogen as gas turbine fuel, J. Eng. Gas Turbines Power 127 (1) (2005) 73–80.
[9] E. Stefan, B. Talic, Y. Larring, A. Gruber, T.A. Peters, Materials challenges in hydrogen-fuelled gas turbines, Int. Mater. Rev. 67 (5) (2022) 461–486.

[10] F. Dabireau, B. Cuenot, O. Vermorel, T. Poinsot, Interaction of flames of H2+O2 with inert walls, Combust. Flame 135 (1–2) (2003) 123–133.
[11] E. Bancalari, P. Chan, I.S. Diakunchak, Advanced hydrogen gas turbine development program, in: Turbo Expo: Power for Land, Sea, and Air, vol. 47918, 2007, pp. 977–987.
[12] C. White, R. Steeper, A.E. Lutz, The hydrogen-fueled internal combustion engine: a technical review, Int. J. Hydrog. Energy 31 (10) (2006) 1292–1305.
[13] L. Qiao, C. Kim, G. Faeth, Suppression effects of diluents on laminar premixed hydrogen/oxygen/nitrogen flames, Combust. Flame 143 (1–2) (2005) 79–96.
[14] C. Yan, M. Bi, Y. Li, W. Gao, Effects of nitrogen and carbon dioxide on hydrogen explosion behaviors near suppression limit, J. Loss Prev. Process. Ind. 67 (2020) 104228.
[15] Y. Yu, H. Qu, P. Ping, Y. Liu, Study on the inhibition of hydrogen explosion using gas-solid two-phase inhibitors, J. Loss Prev. Process. Ind. 92 (2024) 105466.
[16] S. Zhang, X. Wen, Z. Guo, S. Zhang, W. Ji, Effect of N2 and CO2 on explosion behavior of hydrogen-air mixtures in non-premixed state, Fire Saf. J. 138 (2023) 103790.
[17] Z.-m. Luo, F. Nan, F.-m. Cheng, Y. Xiao, T. Wang, R.-k. Li, B. Su, Study on the inhibition of hydrogen explosion pressure and flame propagation by trifluoroiodomethane, Int. J. Hydrog. Energy 49 (2024) 670–680.
[18] M. Gao, M. Bi, L. Ye, Y. Li, H. Jiang, M. Yang, C. Yan, W. Gao, Suppression of hydrogen-air explosions by hydrofluorocarbons, Process. Saf. Environ. Prot. 145 (2021) 378–387.
[19] G. Dixon-Lewis, Mechanism of inhibition of hydrogen-air flames by hydrogen bromide and its relevance to the general problem of flame inhibition, Combust. Flame 36 (1979) 1–14.
[20] G. Dixon-Lewis, P. Marshall, B. Ruscic, A. Burcat, E. Goos, A. Cuoci, A. Frassoldati, T. Faravelli, P. Glarborg, Inhibition of hydrogen oxidation by HBr and Br2, Combust. Flame 159 (2) (2012) 528–540.
[21] M.C. Drake, J.W. Hastie, Temperature profiles of inhibited flames using Raman spectroscopy, Combust. Flame 40 (1981) 201–211.
[22] P. Badhuk, R. Ravikrishna, Flame inhibition by aqueous solution of Alkali salts in methane and LPG laminar diffusion flames, Fire Saf. J. 130 (2022) 103586.
[23] D. Miller, R. Evers, G. Skinner, Effects of various inhibitors on hydrogen-air flame speeds, Combust. Flame 7 (1963) 137–142.
[24] S. Shang, J. Zhang, J. Zhang, T. Luo, M. Bi, H. Jiang, Y. Li, W. Gao, Study on the effect of explosion suppression equipment on hydrogen explosions, J. Loss Prev. Process. Ind. 83 (2023) 105046.
[25] M. Mann, C. Jainski, M. Euler, B. Böhm, A. Dreizler, Transient flame–wall interactions: Experimental analysis using spectroscopic temperature and CO concentration measurements, Combust. Flame 161 (9) (2014) 2371–2386.
[26] K. Kedia, H. Altay, A. Ghoniem, Impact of flame-wall interaction on premixed flame dynamics and transfer function characteristics, Proc. Combust. Inst. 33 (1) (2011) 1113–1120.
[27] T. Poinsot, D.C. Haworth, G. Bruneaux, Direct simulation and modeling of flame-wall interaction for premixed turbulent combustion, Combust. Flame 95 (1–2) (1993) 118–132.
[28] H. Kosaka, F. Zentgraf, A. Scholtissek, C. Hasse, A. Dreizler, Effect of flame-wall interaction on local heat release of methane and DME combustion in a side-wall quenching geometry, Flow, Turbul. Combust. 104 (2020) 1029–1046.
[29] Y. Wang, M. Tanahashi, Three-dimensional geometrical effects on the near-wall quenching of turbulent premixed flame, Proc. Combust. Inst. 40 (1–4) (2024) 105629.
[30] T. Zirwes, T. Häber, F. Zhang, H. Kosaka, A. Dreizler, M. Steinhausen, C. Hasse, A. Stagni, D. Trimis, R. Suntz, et al., Numerical study of quenching distances for side-wall quenching using detailed diffusion and chemistry, Flow Turbul. Combust. 106 (2021) 649–679.
[31] C. Chi, C. Yu, B. Cuenot, U. Maas, D. Thévenin, Effect of differential diffusion on head-on quenching of premixed NH3/H2/air flames within turbulent boundary layers, Proc. Combust. Inst. 40 (1–4) (2024) 105276.
[32] P. Tamadonfar, S. Karimkashi, T. Zirwes, V. Vuorinen, O. Kaario, A numerical study on premixed laminar ammonia/air flames enriched with hydrogen: An analysis on flame–wall interaction, Combust. Flame 265 (2024) 113444.
[33] P. Popp, M. Baum, Analysis of wall heat fluxes, reaction mechanisms, and unburnt hydrocarbons during the head-on quenching of a laminar methane flame, Combust. Flame 108 (3) (1997) 327–348.
[34] T. Häber, R. Suntz, Effect of different wall materials and thermal-barrier coatings on the flame-wall interaction of laminar premixed methane and propane flames, Int. J. Heat Fluid Flow 69 (2018) 95–105.
[35] U. Maas, J. Warnatz, Ignition processes in hydrogen-oxygen mixtures, Combust. Flame 74 (1) (1988) 53–69.
[36] J.O. Hirschfelder, C.F. Curtiss, R.B. Bird, M.G. Mayer, Molecular Theory of Gases and Liquids, vol. 165, Wiley, New York, 1964.
[37] S. Drost, S. Eckart, C. Yu, R. Schießl, H. Krause, U. Maas, Numerical and experimental investigations of CH4/H2 mixtures: ignition delay times, laminar burning velocity and extinction limits, Energies 16 (6) (2023) 2621.
[38] T. Szabó, J. Yáñez, A. Kotchourko, M. Kuznetsov, T. Jordan, Parameterization of laminar burning velocity dependence on pressure and temperature in hydrogen/air/steam mixtures, Combust. Sci. Technol. 184 (10–11) (2012) 1427–1444.
[39] S. Eckart, C. Yu, U. Maas, H. Krause, Experimental and numerical investigations on extinction strain rates in non-premixed counterflow methane and propane flames in an oxygen reduced environment, Fuel 298 (2021) 120781.
[40] C. Wu, Y.-R. Chen, R. Schießl, S.S. Shy, C. Yu, U. Maas, et al., Experimental and numerical investigation of the induced ignition process in ammonia/air and ammonia/hydrogen/air mixtures, Proc. Combust. Inst. 40 (1–4) (2024) 105466.
[41] C. Strassacker, V. Bykov, U. Maas, REDIM reduced modeling of quenching at a cold wall including heterogeneous wall reactions, Int. J. Heat Fluid Flow 69 (2018) 185–193.
[42] C. Strassacker, V. Bykov, U. Maas, REDIM reduced modeling of flame quenching at a cold wall–The influence of detailed transport models and detailed mechanisms, Combust. Sci. Technol. 191 (2) (2019) 208–222.
[43] M. Day, D. Stamp, K. Thompson, G. Dixon-Lewis, Inhibition of hydrogen-air and hydrogen-nitrous oxide flames by halogen compounds, in: Symposium (International) on Combustion, vol. 13, Elsevier, 1971, pp. 705–712, 1.
[44] C. Strassacker, V. Bykov, U. Maas, Reduced modeling of flame-wall-interactions of premixed isooctane-air systems including detailed transport and surface reactions, Proc. Combust. Inst. 38 (1) (2021) 1063–1070.